

Role of the $N^*(1535)$ in $pp \rightarrow pp\phi$ and $\pi^- p \rightarrow n\phi$ reactions

Ju-Jun Xie,^{1,2,*} Bing-Song Zou,^{1,2,3,†} and Huan-Ching Chiang^{1,3,4}

¹*Institute of High Energy Physics, CAS, Beijing 100049, People's Republic of China*

²*Graduate University of Chinese Academy of Sciences, Beijing 100049, People's Republic of China*

³*Center of Theoretical Nuclear Physics, National Laboratory of Heavy Ion Accelerator, Lanzhou 730000, People's Republic of China*

⁴*Department of Physics, South-west University, Chongqing 400071, People's Republic of China*

(Received 29 May 2007; published 22 January 2008)

The near-threshold ϕ -meson production in proton-proton and $\pi^- p$ collisions is studied with the assumption that the production mechanism is due to the sub- $N\phi$ -threshold $N^*(1535)$ resonance. The π^0 -, η -, and ρ^0 -meson exchanges for proton-proton collisions are considered. It is shown that the contribution to the $pp \rightarrow pp\phi$ reaction from the t -channel π^0 -meson exchange is dominant. With a significant $N^*(1535)N\phi$ coupling [$g_{N^*(1535)N\phi}^2/4\pi = 0.13$], both $pp \rightarrow pp\phi$ and $\pi^- p \rightarrow n\phi$ data are very well reproduced. The significant coupling of the $N^*(1535)$ resonance to $N\phi$ is compatible with previous indications of a large $s\bar{s}$ component in the quark wave function of the $N^*(1535)$ resonance and may be the real origin of the significant enhancement of the ϕ production over the naive OZI-rule predictions.

DOI: 10.1103/PhysRevC.77.015206

PACS number(s): 13.75.-n, 14.20.Gk, 13.30.Eg

I. INTRODUCTION

The meson production reaction in nucleon-nucleon collisions near threshold has the potential to gain new information on hadron properties [1], and the experimental database on meson production in nucleon-nucleon collisions has expanded significantly in recent years. However, the study of the strangeness content of the quark wave functions of baryons and baryon resonances, not only experimentally but also theoretically, has been an interesting area [2] that is expected to provide new information on the configuration of baryons and baryon resonances. In the naive quark model, the nucleon and nucleon resonances have no strangeness contents, whereas the ϕ meson is an ideally mixed pure $s\bar{s}$ state. From the point of view of the naive quark model the $pp \rightarrow pp\phi$ reaction involves disconnected quark lines and is an Okubo-Zweig-Iizuka (OZI) rule [3] suppressed process. The study of ϕ -meson production in nucleon-nucleon reactions may provide information on the strangeness degrees of freedom in the nucleon or nucleon resonances and is of importance both experimentally and theoretically.

Several years ago, the exclusive production cross section for ϕ -meson production in pp collisions at $P_{\text{lab}} = 3.67$ GeV/ c was measured by the DISTO Collaboration [4], and the preliminary result at an excess energy of 18.5 MeV above the threshold was also published by the ANKE group [5]. With this experimental information about this reaction, several theoretical articles [6–9] were published to try to explain the experimental data by using various models. Recently, more data at other energies are available from the ANKE facility [10]. Comparing the data for the ω -meson production from literature, a significant enhancement of a ϕ/ω ratio of a factor 8 is found compared to predictions based on the OZI rule. This findings require more theoretical work to understand its origin.

It is well known that the $N^*(1535)$ resonance couples strongly to the ηN channel. Recently, it was found that the $N^*(1535)$ resonance has a significant coupling to $K\Lambda$ in the analysis of the $J/\psi \rightarrow \bar{p}\Lambda K^+$ decay and the $pp \rightarrow p\Lambda K^+$ reaction near threshold [11]. The analyses [12,13] of the recent SAPHIR and CLAS $\gamma p \rightarrow K^+\Lambda$ data [14,15] also show a large coupling of the $N^*(1535)$ to $K\Lambda$. In a chiral unitary coupled-channels approach it was found that the $N^*(1535)$ resonance is dynamically generated as a pole in the second Riemann sheet with its mass, width, and branching ratios in fair agreement with experiments and the couplings of the $N^*(1535)$ resonance to $K\Sigma$, ηN , and $K\Lambda$ are large compared to the πN channel [16]. The analyses of data on the η' photoproduction on the proton for photon energies from 1.527 to 2.227 GeV also suggest the coupling of the $\eta' N$ channel to the $N^*(1535)$ resonance [17].

From the naive quark model, both η mesons and η' mesons have a $s\bar{s}$ component. It seems that the $N^*(1535)$ couples strongly to mesons with strangeness or with $s\bar{s}$ components. These phenomena indicate that there may be a significant $s\bar{s}$ configuration in the quark wave function of the $N^*(1535)$ resonance. So, we expect that the $N^*(1535)$ resonance may also have a significant coupling to the ϕN channel.

In this article, we assume that the productions of the ϕ meson in proton-proton and $\pi^- p$ collisions are predominantly through the excitation and decay of the sub- ϕN -threshold $N^*(1535)$ resonance. By using this picture, we calculate the $pp \rightarrow pp\phi$ and $\pi^- p \rightarrow n\phi$ reactions in the framework of an effective Lagrangian approach. By comparing with the experimental data we find that the coupling of the $N^*(1535)$ resonance to the ϕN channel needs to be somewhat larger than its the coupling to $N\rho$ channel. The significant coupling of the $N^*(1535)$ resonance to $N\phi$ is compatible with previous indications of a large $s\bar{s}$ component in the quark wave function of the $N^*(1535)$ resonance and may be the real origin of the significant enhancement of the ϕ production over the naive OZI rule predictions.

* xiejun@mail.ihep.ac.cn

† zoubs@mail.ihep.ac.cn

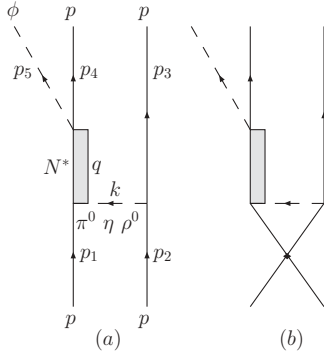


FIG. 1. Feynman diagrams for the $pp \rightarrow pp\phi$ reaction. The diagram on the left shows the direct process, whereas that on the right shows the exchange one. p_i ($i = 1, 2, 3, 4, 5$) stands for the four-momenta of the initial and final particle; k and q stand for the four-momenta of exchange meson and the intermediate resonance [$N^*(1535)$], respectively.

In the next section, we will give the formalism and ingredients in our calculation, and then numerical results and discussions are given in Sec. III. A short summary is given in the last section.

II. FORMALISM AND INGREDIENTS

We study the $pp \rightarrow pp\phi$ and $\pi^- p \rightarrow n\phi$ reactions near threshold in an effective Lagrangian approach. We assume that the near-threshold ϕ productions in proton-proton and $\pi^- p$ collisions are through the intermediate excitation of the sub- ϕN -threshold $N^*(1535)$ resonance. The π^0 -, η -, and ρ^0 -meson exchanges are considered for proton-proton collisions. The basic Feynman diagrams for the $pp \rightarrow pp\phi$ reaction and the s -channel diagram for the $\pi^- p \rightarrow n\phi$ reaction are depicted in Figs. 1 and 2, respectively.

We use the commonly used interaction Lagrangians for πNN , ηNN , and ρNN couplings,

$$\mathcal{L}_{\pi NN} = -ig_{\pi NN} \bar{u}_N \gamma_5 \vec{\tau} \cdot \vec{\pi} u_N, \quad (1)$$

$$\mathcal{L}_{\eta NN} = -ig_{\eta NN} \bar{u}_N \gamma_5 \eta u_N, \quad (2)$$

$$\mathcal{L}_{\rho NN} = -g_{\rho NN} \bar{u}_N \left(\gamma_\mu + \frac{\kappa}{2m_N} \sigma_{\mu\nu} \partial^\nu \right) \vec{\tau} \cdot \vec{\rho}^\mu u_N. \quad (3)$$

At each vertex a relevant off-shell form factor is used. In our computation, we take the same form factors as that used

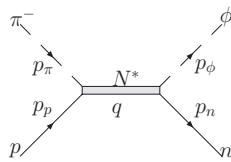


FIG. 2. Feynman diagram for $\pi^- p \rightarrow n\phi$ reaction. p_π , p_p , p_ϕ , p_n , and q stand for the four-momenta of π^- , proton, ϕ , neutron, and intermediate resonance [$N^*(1535)$], respectively.

in the well-known Bonn potential model [18]

$$F_M^{NN}(k_M^2) = \left(\frac{\Lambda_M^2 - m_M^2}{\Lambda_M^2 - k_M^2} \right)^n, \quad (4)$$

with $n = 1$ for π^0 and η mesons and $n = 2$ for ρ^0 mesons. k_M , m_M , and Λ_M are the four-momentum, mass, and cut-off parameters for the exchanged meson (M), respectively. The coupling constants and the cut-off parameters are taken as [18–20]: $g_{\pi NN}^2/4\pi = 14.4$, $g_{\rho NN}^2/4\pi = 0.9$, $\Lambda_\pi = \Lambda_\eta = 1.3$ GeV, $\Lambda_\rho = 1.6$ GeV, and $\kappa = 6.1$. The value of ηNN coupling constant is extremely uncertain, with values of $g_{\eta NN}^2/4\pi$ between 0 and 7 being quoted in the literature, we use $g_{\eta NN}^2/4\pi = 0.4$ because many authors say that it is small (see, e.g., Refs. [21,22]).

To calculate the invariant amplitudes of diagrams in Fig. 1 and Fig. 2 with the $N^*(1535)$ resonance model, we also need to know the interaction Lagrangians involving the $N^*(1535)$ resonance. In Ref. [23], a Lorentz covariant orbital-spin (L-S) scheme for N^*NM couplings has been illustrated in detail. With this scheme, we can easily write the effective $N^*(1535)N\pi$, $N^*(1535)N\eta$, $N^*(1535)N\rho$, and $N^*(1535)N\phi$ couplings,

$$\mathcal{L}_{\pi NN^*} = ig_{N^*N\pi} \bar{u}_N u_{N^*} + \text{h.c.}, \quad (5)$$

$$\mathcal{L}_{\eta NN^*} = ig_{N^*N\eta} \bar{u}_N u_{N^*} + \text{h.c.}, \quad (6)$$

$$\mathcal{L}_{\rho NN^*} = ig_{N^*N\rho} \bar{u}_N \gamma_5 \left(\gamma_\mu - \frac{q_\mu \gamma^\nu q_\nu}{q^2} \right) \varepsilon^\mu(p_\rho) u_{N^*} + \text{h.c.}, \quad (7)$$

$$\mathcal{L}_{\phi NN^*} = ig_{N^*N\phi} \bar{u}_N \gamma_5 \left(\gamma_\mu - \frac{q_\mu \gamma^\nu q_\nu}{q^2} \right) \varepsilon^\mu(p_\phi) u_{N^*} + \text{h.c.} \quad (8)$$

Here u_N and u_{N^*} are the spin wave functions for the nucleon and $N^*(1535)$ resonance; $\varepsilon^\mu(p_\rho)$ and $\varepsilon^\mu(p_\phi)$ are the polarization vectors of the ρ and ϕ mesons, respectively. It is worth noting that because the spins of the ρ meson and ϕ meson are 1, both S -wave and D -wave L-S couplings are possible for the $N^*(1535)N\rho$ and $N^*(1535)N\phi$ interactions. It was found that the S -wave coupling has a significant contribution to the partial decay width of the $N^*(1535)$ resonance compared with the D wave [24,25]. In our calculation we consider only the S -wave $N^*(1535)$ resonance couplings to $N\rho$ and neglect the D -wave $N^*(1535)$ resonance couplings to $N\phi$ for simplicity. The monopole form factors for $N^*(1535) - N$ -meson vertices are used,

$$F_M^{N^*N}(k_M^2) = \frac{\Lambda_M^{*2} - m_M^2}{\Lambda_M^{*2} - k_M^2}, \quad (9)$$

with $\Lambda_\pi^* = \Lambda_\eta^* = \Lambda_\rho^* = 1.3$ GeV.

The $N^*(1535)N\pi$, $N^*(1535)N\eta$, and $N^*(1535)N\rho$ coupling constants are determined from the experimentally observed partial decay widths of the $N^*(1535)$ resonance. With the effective interaction Lagrangians described by Eq. (5) and Eq. (6), the partial decay widths $\Gamma_{N^*(1535) \rightarrow N\pi}$ and $\Gamma_{N^*(1535) \rightarrow N\eta}$ can be easily calculated [24]. The coupling

constants are related to the partial decay widths,

$$\Gamma_{N^*(1535) \rightarrow N\pi} = \frac{3g_{N^*N\pi}^2(m_N + E_N^\pi)p_\pi^{\text{c.m.}}}{4\pi M_{N^*}}, \quad (10)$$

$$\Gamma_{N^*(1535) \rightarrow N\eta} = \frac{g_{N^*N\eta}^2(m_N + E_N^\eta)p_\eta^{\text{c.m.}}}{4\pi M_{N^*}}, \quad (11)$$

where

$$p_{\pi/\eta}^{\text{c.m.}} = \sqrt{\frac{[M_{N^*}^2 - (m_N + m_{\pi/\eta})^2][M_{N^*}^2 - (m_N - m_{\pi/\eta})^2]}{4M_{N^*}^2}}, \quad (12)$$

and

$$E_N^{\pi/\eta} = \sqrt{(p_{\pi/\eta}^{\text{c.m.}})^2 + m_N^2}. \quad (13)$$

For the $N^*(1535)N\rho$ coupling constant, we get it from the partial decay width $\Gamma_{N^*(1535) \rightarrow N\rho \rightarrow N\pi\pi}$, and the partial decay width can be evaluated from the total invariant amplitude $\mathcal{M}_{N^*(1535) \rightarrow N\rho \rightarrow N\pi\pi}$ of the $N^*(1535) \rightarrow N\rho \rightarrow N\pi\pi$ decay and a three-body phase-space integration,

$$\begin{aligned} \mathcal{M}_{N^*(1535) \rightarrow N\rho \rightarrow N\pi\pi} &= g_{\rho\pi\pi} g_{N^*(1535)N\rho} F_\rho^{N^*N}(k_\rho^2) \bar{u}_N(p_1, s_1) \\ &\times \gamma_5 \left(\gamma_\mu - \frac{q_\mu \gamma^\sigma q_\sigma}{q^2} \right) \\ &\times G_\rho^{\mu\nu}(k_\rho)(p_2 - p_3)_\nu u_{N^*}(q, s_{N^*}), \end{aligned} \quad (14)$$

$$\begin{aligned} d\Gamma_{N^*(1535) \rightarrow N\rho \rightarrow N\pi\pi} &= \frac{|\mathcal{M}_{N^*(1535) \rightarrow N\rho \rightarrow N\pi\pi}|^2 d^3p_1 m_1 d^3p_2}{(2\pi)^3 E_1 (2\pi)^3 2E_2} \frac{1}{(2\pi)^3} \frac{d^3p_3}{2E_3} \\ &\times (2\pi)^4 \delta^4(q - p_1 - p_2 - p_3), \end{aligned} \quad (15)$$

where $G_\rho^{\mu\nu}(k_\rho)$ is the propagator of the ρ meson with the form

$$G_\rho^{\mu\nu}(k_\rho) = -i \left(\frac{g^{\mu\nu} - k_\rho^\mu k_\rho^\nu / k_\rho^2}{k_\rho^2 - m_\rho^2} \right). \quad (16)$$

Here q and k_ρ are the four-momenta of the $N^*(1535)$ resonance and the intermediate ρ meson; p_1, m_1 , and E_1 stand for the four-momentum, mass, and energy of the nucleon; s_1 and s_{N^*} the spin projection of the nucleon and the $N^*(1535)$ resonance; and $p_{2/3}$ and $E_{2/3}$ stand for the four-momentum and energy of the final two pions, respectively. In our calculation, we use $g_{\rho\pi\pi}^2/4\pi = 2.91$ as the same as that used in Ref. [26].

There is no information for the coupling constant of the $N^*(1535)N\phi$ vertex. We determine it from the $\pi^- p \rightarrow n\phi$ reaction. We assume that the near-threshold ϕ production in $\pi^- p$ collisions is through the intermediate excitation of the sub- ϕN -threshold $N^*(1535)$ resonance. Then, by comparing the theoretical total cross sections of $\pi^- p \rightarrow n\phi$ reaction with experimental data, we can extract the $N^*(1535)N\phi$ coupling constant.

In Fig 2, we show the s -channel diagram for the $\pi^- p \rightarrow n\phi$ reaction, the intermediate excitation is a sub- $n\phi$ -threshold $N^*(1535)$ resonance. Following the Feynman rules and with the above formula, we can obtain the invariant amplitude \mathcal{A} of

the $\pi^- p \rightarrow n\phi$ reaction,

$$\begin{aligned} \mathcal{A} &= g_{N^*N\pi} g_{N^*N\phi} F_{N^*}(q^2) \bar{u}(p_n, s_n) \gamma_5 \left(\gamma_\mu - \frac{q_\mu \gamma^\nu q_\nu}{q^2} \right) \\ &\times \varepsilon^\mu(p_\phi, s_\phi) G_{N^*(1535)}(q) u(p_p, s_p), \end{aligned} \quad (17)$$

with s_n, s_p, s_ϕ as the spin projection of the ϕ meson and the nucleon, respectively. The form factor for $N^*(1535)$ resonance, $F_{N^*}(q^2)$, is taken as in Refs. [12,27]

$$F_{N^*}(q^2) = \frac{\Lambda^4}{\Lambda^4 + [q^2 - M_{N^*(1535)}^2]^2}, \quad (18)$$

with $\Lambda = 2.0$ GeV. $G_{N^*(1535)}(q)$ is the propagator of the $N^*(1535)$ resonance, which can be written in a Breit-Wigner form [28],

$$G_{N^*(1535)}(q) = \frac{\gamma q + M_{N^*(1535)}}{q^2 - M_{N^*(1535)}^2 + i M_{N^*(1535)} \Gamma_{N^*(1535)}(s)}. \quad (19)$$

Here $\Gamma_{N^*(1535)}(s)$ is the energy-dependent total width of the $N^*(1535)$ resonance. According to PDG [24], the dominant decay channels for the $N^*(1535)$ resonance are πN and ηN , so we take

$$\begin{aligned} \Gamma_{N^*(1535)}(s) &= \Gamma_{N^*(1535) \rightarrow N\pi} \frac{\rho_{\pi N}(s)}{\rho_{\pi N}[M_{N^*(1535)}^2]} \\ &+ \Gamma_{N^*(1535) \rightarrow N\eta} \frac{\rho_{\eta N}(s)}{\rho_{\eta N}[M_{N^*(1535)}^2]}, \end{aligned} \quad (20)$$

where $\rho_{\pi(\eta)N}(s)$ is the following two-body phase-space factor,

$$\begin{aligned} \rho_{\pi(\eta)N}(s) &= \frac{2p_{\pi(\eta)N}^{\text{c.m.}}(s)}{\sqrt{s}} \\ &= \frac{\sqrt{\{s - [m_N + m_{\pi(\eta)}]^2\} \{s - [m_N - m_{\pi(\eta)}]^2\}}}{s}. \end{aligned} \quad (21)$$

From the amplitude, we can easily obtain the total cross sections of the $\pi^- p \rightarrow n\phi$ reaction as functions of the excess energies. By adjusting the $N^*(1535)N\phi$ coupling constant, we can compare the theoretical results with the experimental data. Theoretical results with $g_{N^*(1535)N\phi}^2/4\pi = 0.13$ are compared with the experimental data by the solid curve in Fig. 3 (left); we find an excellent agreement between our results and the experimental data. Contributions from the u -channel N^* exchange and ρ -meson exchange between the pion and the proton are also checked and are found to be negligible.

With experimental mass (1535 MeV), width (150 MeV), branching ratios of the $N^*(1535)$ [24], and the total cross sections of the $\pi^- p \rightarrow n\phi$ reaction, we obtain all the coupling constants as listed in Table I.

Aside from the $N^*(1535)$, there are other resonances that have decay branching ratios to the $N\eta$ channel for the mass range of 1.6–2.1 GeV, i.e., $N^*(1650)$, $N^*(1710)$, $N^*(1720)$, $N^*(1900)$, $N^*(2080)$, and $N^*(2100)$ [24]. They may also have some $s\bar{s}$ components and hence have decay branching ratios to $N\phi$. So we also tried to use these resonances to get fits to the $\pi^- p \rightarrow n\phi$ data by adjusting their coupling constants to $N\phi$ and off-shell form factor parameters. The best fits with

TABLE I. Relevant $N^*(1535)$ parameters.

Decay channel	Branching ratios	Adopted branching ratios	$g^2/4\pi$
$N\pi$	0.35–0.55	0.45	0.033
$N\eta$	0.45–0.60	0.53	0.28
$N\rho \rightarrow N\pi\pi$	0.02 ± 0.01	0.02	0.10
$N\phi$	–	–	0.13

$N^*(1650)$, $N^*(1710)$, $N^*(1720)$, and $N^*(1900)$ are shown in Fig. 3 (left) by dotted, dashed, short-dashed, and dot-dashed curves, respectively. The fits with $N^*(2080)$ and $N^*(2100)$ are worse and not shown here. Except the fit with $N^*(1650)$, all other fits underestimate the first data point by a factor more than 2. This is because $N^*(1710)$, $N^*(1720)$, and $N^*(1900)$ have positive parity and decay to $n\phi$ in relative P wave, which gives a strong near-threshold suppression. The negative-parity $N^*(1650)$ decays to $n\phi$ in relative S wave, hence reproduces the data near threshold as good as the $N^*(1535)$ but worse for the data point at the highest energy. In addition to the fact that the $N^*(1535)$ gives the best fit to the data, there are two more points favoring the dominance of the $N^*(1535)$ contribution. First, unlike the ϕ meson with nearly only the $s\bar{s}$ component, the η meson has rather similar amount of $s\bar{s}$ and $u\bar{u} + d\bar{d}$ components. Even for N^* resonances without any $s\bar{s}$ components, they can still couple to the $N\eta$ channel through the $u\bar{u} + d\bar{d}$ components of η without violating OZI rule. Only $N^*(1535)$ has an extraordinary large coupling to $N\eta$ [24] and $K\Lambda$ [11], which indicate significantly large $s\bar{s}$ components inside the resonance. All other N^* resonances have smaller couplings to $N\eta$ than to $N\pi$, especially the $N^*(1650)$. Second, the $N^*(1710)$, $N^*(1900)$, $N^*(2080)$, and $N^*(2100)$ are not well-established resonances yet [24].

Although the single $N^*(1535)$ dominance model already reproduces the data very well with $\chi^2 = 4.7$ for nine data points, we cannot exclude alternative solutions with significant contributions from other N^* resonances. For example, if we include two resonances to fit the data, the combination of 70% $N^*(1535)$ and 30% $N^*(1900)$ will give the best fit to the data as shown by the solid curve in Fig. 3 (right) with $\chi^2 = 2.5$. In the fit, the contributions from $N^*(1535)$ and $N^*(1900)$ are added incoherently. The further inclusion of $N^*(1650)$

does not improve the fit and results in zero contribution from the $N^*(1650)$. However, if we exclude the contribution from $N^*(1535)$, the combination of 56% $N^*(1650)$ and 44% $N^*(1900)$ also gives a quite good fit to the data with $\chi^2 = 4.5$ for the nine data points.

Because a recent study [25] gives a very weak coupling of $N^*(1650)$ to $N\rho$, from SU(3) symmetry, a weak coupling of $N^*(1650)$ to $N\phi$ would also be expected. So in the following we consider only the dominant contribution from the $N^*(1535)$.

For the $pp \rightarrow pp\phi$ reaction, the full invariant amplitude in our calculation is composed of three parts corresponding to the $N^*(1535)$ resonance production from π^0- , $\eta-$, and ρ^0 -meson exchanges, respectively:

$$\mathcal{M} = \sum_{i=\pi,\eta,\rho} \mathcal{M}_i. \quad (22)$$

Each amplitude can be obtained straightforwardly with the effective couplings and following the Feynman rules. Here we give explicitly the amplitude \mathcal{M}_π , as an example,

$$\begin{aligned} \mathcal{M}_\pi &= g_{\pi NN} g_{N^* N \pi} g_{N^* N \phi} F_\pi^{NN}(k_\pi^2) F_\pi^{N^* N}(k_\pi^2) F_{N^*}(q^2) \\ &\times \varepsilon^\mu(p_\phi, s_\phi) G_\pi(k_\pi) \bar{u}(p_4, s_4) \gamma_5 \left(\gamma_\mu - \frac{q_\mu \gamma^\nu q_\nu}{q^2} \right) \\ &\times G_{N^*(1535)}(q) u(p_1, s_1) \bar{u}(p_3, s_3) \gamma_5 u(p_2, s_2) \\ &+ (\text{exchange term with } p_1 \leftrightarrow p_2), \end{aligned} \quad (23)$$

where s_ϕ is the spin projection of the ϕ meson and s_i ($i = 1, 2, 3, 4$) and p_i ($i = 1, 2, 3, 4$) represent the spin projection and four-momenta of the two initial and two final protons, respectively. $G_\pi(k_\pi)$ is the pion meson propagator,

$$G_\pi(k_\pi) = \frac{i}{k_\pi^2 - m_\pi^2}. \quad (24)$$

The final-state interaction (FSI) enhancement factor in the 1S_0 diproton state is taken into account by means of the general framework based on the Jost function formalism [30] with

$$|J(q)|^{-1} = \frac{k + i\beta}{k - i\alpha}, \quad (25)$$

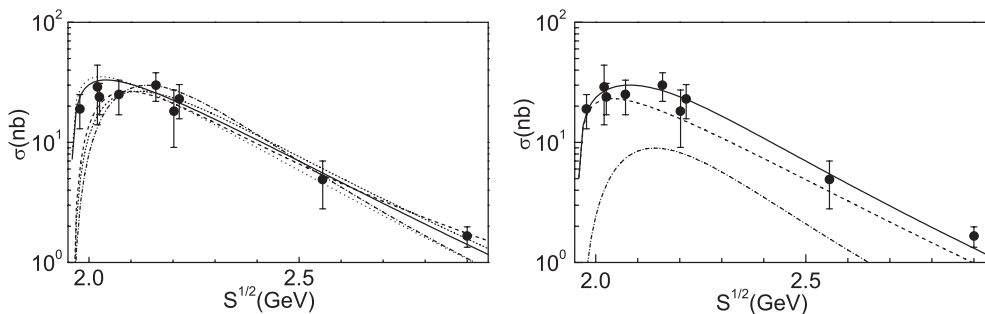


FIG. 3. Total cross sections vs the center-of-mass (c.m.) energy $S^{1/2}$ for $\pi^- p \rightarrow n\phi$ reactions with data from Ref. [29]. (Left) The best fits with $N^*(1535)$ (solid), $N^*(1650)$ (dotted), $N^*(1710)$ (dashed), $N^*(1720)$ (short-dashed), and $N^*(1900)$ (dot-dashed), respectively; (right) fit (solid) with $N^*(1535)$ (dashed) plus $N^*(1900)$ (dot-dashed).

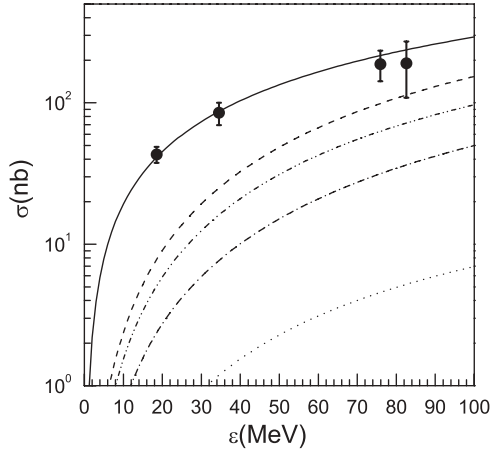


FIG. 4. Total cross sections vs. excess energies (ε) for the $pp \rightarrow pp\phi$ reaction from present calculation are compared with experimental data [4,10]. The double dotted-dashed, dotted, dashed-dotted, and dashed curves stand for contributions from π^0 -, η -, and ρ^0 -meson exchanges and their simple sum, respectively. Solid line corresponds to the results with the 1S_0 pp FSI.

where k is the internal momentum of pp subsystem, and the α and β are related to the scattering parameters via

$$a = \frac{\alpha + \beta}{\alpha\beta}, \quad r = \frac{2}{\alpha + \beta}, \quad (26)$$

with $\alpha = -20.5$ MeV/ c and $\beta = 166.7$ MeV/ c [6] (i.e., $a = -7.82$ fm and $r = 2.79$ fm) in the present study.

Then the calculations of the differential and total cross sections are straightforward,

$$d\sigma(pp \rightarrow pp\phi) = \frac{1}{4} \frac{m_p^2}{F} \sum_{s_i} \sum_{s_f} |\mathcal{M}|^2 \frac{m_p d^3 p_3}{E_3} \frac{m_p d^3 p_4}{E_4} \frac{d^3 p_5}{2E_5} \times \delta^4(p_1 + p_2 - p_3 - p_4 - p_5), \quad (27)$$

with the flux factor

$$F = (2\pi)^5 \sqrt{(p_1 \times p_2)^2 - m_p^4}. \quad (28)$$

Because the relative phases among different meson exchanges in the amplitude of Eq. (22) are not known, the interference terms are ignored in our concrete calculations.

III. NUMERICAL RESULTS AND DISCUSSIONS

With the formalism and ingredients given above, the total cross section versus excess energy ε for the $pp \rightarrow pp\phi$ reaction is calculated by using a Monte Carlo multiparticle phase space integration program. It is known that the near-threshold production of the η meson in $pp \rightarrow pp\eta$ reaction is thought to occur predominantly via the excitation of the $N^*(1535)$ resonance. However, the excitation mechanism of the $N^*(1535)$ resonance in proton-proton collisions is currently still debated. For example, Batinić *et al.* [31] and Nakayama [32] have found that the π - and η -meson exchanges between two protons play dominant roles for the excitation of the $N^*(1535)$ resonance. However, Gedalin *et al.* [33] and Fäldt and Wilkin [22] have found that the ρ -meson exchange is the dominant excitation mechanism of the $N^*(1535)$ resonance. Here the π^0 -, η -, and ρ^0 -meson exchanges for $N^*(1535)$ excitation are all considered. By using

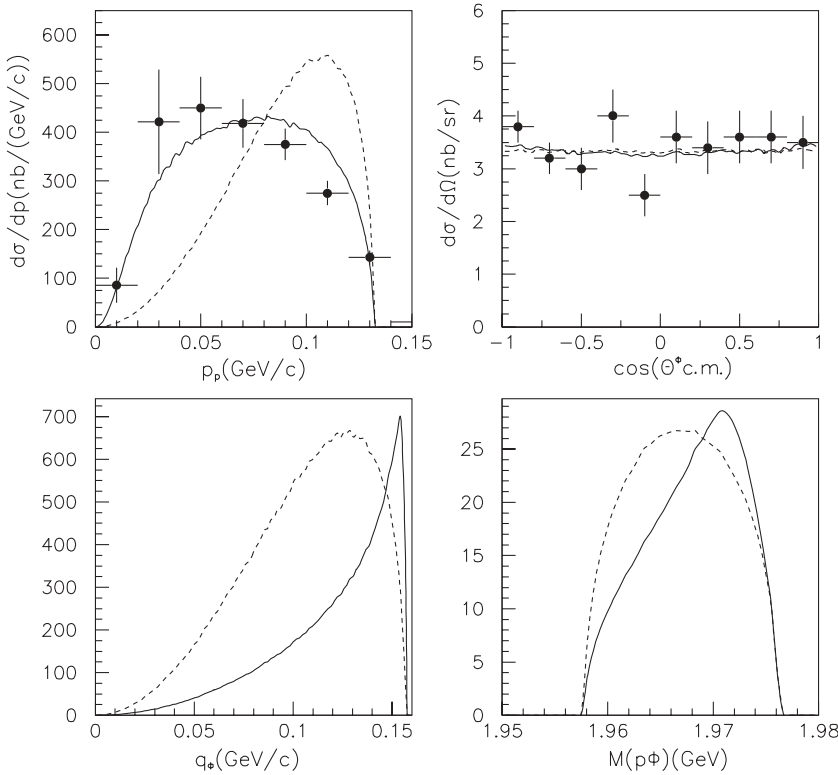


FIG. 5. Differential cross sections (solid lines) for the $pp \rightarrow pp\phi$ reaction at the excess energy $\varepsilon = 18.5$ MeV compared with the ANKE data [5] and phase-space distribution (dashed lines). The upper left panel is the momentum distribution of the outgoing proton. The upper right panel is the angular distribution of the ϕ meson in the total center-of-mass frame; the lower left panel is the distribution of the center-of-mass momentum of the ϕ meson; the lower right panel is the invariant mass spectrum of the outgoing proton and the ϕ meson.

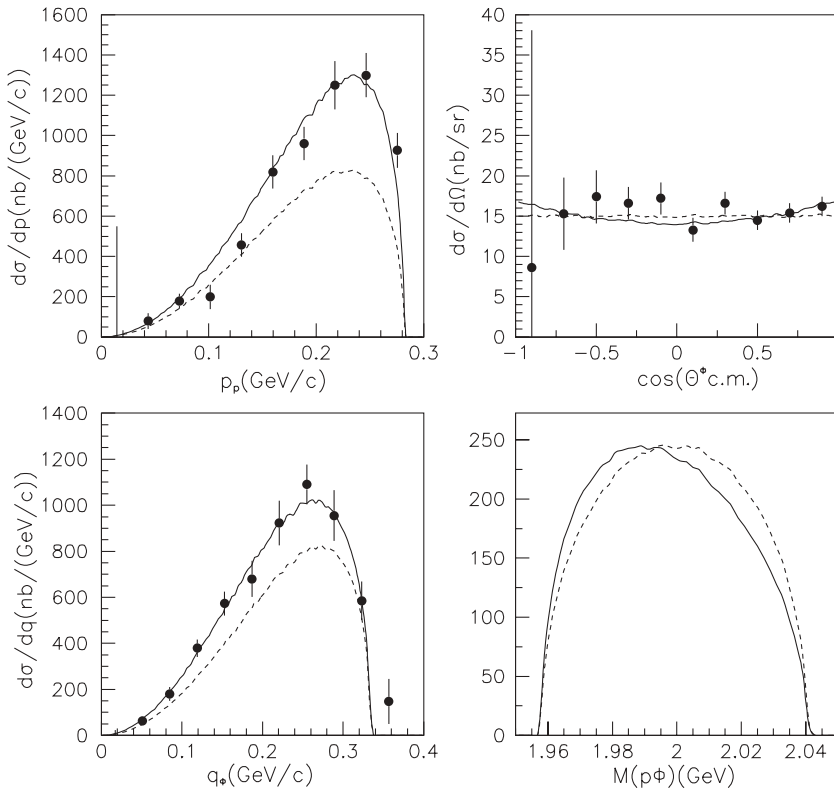


FIG. 6. Differential cross sections for the $pp \rightarrow pp\phi$ reaction at the excess energy $\varepsilon = 83$ MeV compared with the DISTO data [4]. The dashed line reflects pure phase space, whereas the solid lines, which includes the amplitudes but without the pp FSI.

the formalism and ingredients described in Sec. III we first study the roles of different meson exchanges in the $pp \rightarrow pp\phi$ reaction. Our calculated results are shown in Fig. 4 together with the experimental data. The double-dotted-dashed, dotted, and dashed-dotted curves stand for contributions without the pp FSI from π^0 -, η -, and ρ^0 -meson exchanges, respectively. A simple summation of them is shown by the dashed line. One can see that the contribution from the t -channel π^0 -meson exchange is dominant to the $pp \rightarrow pp\phi$ reaction in our model. The ρ^0 -meson exchange has a significant contribution to this reaction, whereas the contribution from the η -meson exchange is negligible.

From Fig. 4 we can see that our theoretical result without the pp FSI agrees well with the experimental data at excess energy $\varepsilon = 83.0$ MeV. However, at lower excess energies such as $\varepsilon = 18.5, 34.5$ MeV, the calculated total cross sections are lower than the data by a factor of more than 4. It is known that the proton-proton FSI plays an important role for the near-threshold meson production in proton-proton collisions. We also include the effect of the $^1S_0 pp$ FSI by using the Jost-function method [30] in our calculation; the results are shown in Fig. 4 by the solid line, which can reproduce the ANKE total cross section data well.

The momentum, angular distributions of the ϕ meson, and the $p\phi$ invariant mass spectrum for the $pp \rightarrow pp\phi$ reaction at excess energy $\varepsilon = 18.5$ and 83.0 MeV are also calculated. In Fig. 5 we present our calculated results at excess energy $\varepsilon = 18.5$ MeV together with experimental data from the ANKE group. Differential cross sections as a function of the center-of-mass (c.m.) momentum of the outgoing proton are presented in the upper left panel. The upper right panel is the angular distribution of the ϕ meson in the total proton-

proton center-of-mass frame. The dashed lines are pure phase-space distributions, whereas the solid lines are full calculations from our model with the $^1S_0 pp$ FSI enhancement factor. By comparing with the data, we find that the pp FSI plays an important role. Our model can explain the experimental data well. In the lower part of Fig. 5 the momentum distribution of the ϕ meson and the invariant mass spectrum of the outgoing proton and the ϕ meson are shown.

In Fig. 6, we present our calculated differential distributions at excess energy $\varepsilon = 83.0$ MeV together with experimental data from the DISTO group. From our calculation we find that there is no need to consider the pp FSI at this energy. An excellent agreement between our model calculation and the experimental data both in shapes and magnitudes can be achieved without taking the pp FSI into account. This is consistent with ANKE findings at $\varepsilon = 75.9$ MeV. The phenomena may suggest that at excess energy about 80 MeV the contribution from pp higher partial waves has already overtaken the 1S_0 partial wave as the dominant contribution and the FSI becomes unimportant.

In our calculation we include only the contribution of the $N^*(1535)$ in the intermediate state. In previous calculations [6–9], the $\pi p \rightarrow \phi N$ through t -channel ρ exchange and/or subthreshold nucleon pole contributions are assumed to be dominant. However, these contributions are very sensitive to the choice of off-shell form factors for the t -channel ρ exchange and the $g_{NN\phi}$ couplings and can be reduced by orders of magnitude within the uncertainties of these ingredients. Considering the ample evidence for large coupling of the $N^*(1535)$ to the strangeness [11–13,16,34] and the $N^*(1535)$ resonance is closer than the nucleon pole to the ϕN threshold, it is more likely that the $N^*(1535)$ plays dominant role for near

threshold ϕ production from πp and pp collisions instead of the nucleon pole or the OZI-suppressed $\phi\rho\pi$ coupling. Our calculation with the $N^*(1535)$ domination reproduces energy dependence of the $\pi^- p \rightarrow \phi n$ and $pp \rightarrow pp\phi$ cross sections better than previous calculations. The significant coupling of the $N^*(1535)$ resonance to $N\phi$ may be the real origin of the significant enhancement of the ϕ production from πp and pp reactions over the naive OZI rule predictions. This makes it difficult to extract the properties of the strangeness in the nucleon from these reactions proposed by J. Ellis *et al.* [35]. There are also some suggestions [36,37] for possible existence of an $N\phi$ bound state just below the $N\phi$ threshold. However, the contribution of such a bound state with width less than 100 MeV will give a much sharper dropping structure for the $\pi^- p \rightarrow \phi n$ cross section at energies near threshold. If such a $N\phi$ bound state does exist, it should have weak coupling to πN and provide only a small contribution to the $\pi^- p \rightarrow \phi n$ reaction.

IV. CONCLUSIONS

In this article, the near-threshold ϕ -meson productions in proton-proton and $\pi^- p$ collisions are studied with an effective Lagrangian approach. We assume that the production mechanism is due to the excitation of the sub- $N\phi$ -threshold $N^*(1535)$ resonance following π^0 -, η -, and ρ^0 -meson exchanges between two protons. $\pi^0 NN$, ηNN , and $\rho^0 NN$ coupling constants (except $g_{\eta NN}$) and form factors are taken from the Bonn potential model. $N^*(1535)N\pi^0$, $N^*(1535)N\eta$, and $N^*(1535)N\rho^0$ coupling constants are determined from the partial decay widths of the $N^*(1535)$ resonance. The $N^*(1535)N\phi$ coupling constant is deduced from a fit to the experimental total cross sections of the $\pi^- p \rightarrow n\phi$ reaction near threshold with the $N^*(1535)$

resonance model. We find that the $N^*(1535)$ resonance has a significant coupling to $N\phi$ [$g_{N^*(1535)N\phi}^2/4\pi = 0.13$].

The total reaction cross sections and differential distributions of the near-threshold $pp \rightarrow pp\phi$ reaction are calculated with the $N^*(1535)$ resonance model without adjustable parameter. Our theoretical calculation agrees quite well with experiments near threshold. We find that the contribution from the t -channel π^0 -meson exchange is dominant to the $pp \rightarrow pp\phi$ reaction.

The significant coupling of the $N^*(1535)$ resonance to the ϕN channel together with the earlier findings of large couplings of the $N^*(1535)$ resonance to the ηN , $\eta' N$, and $K\Lambda$ channels [11–13,17,24] gives a coherent picture that there is a large component of strangeness in the $N^*(1535)$ resonance as expected by various theoretical approaches [11,16,34,38]. It also gives a natural explanation for the significant enhancement of the ϕ production from πp and pp reactions over the naive OZI rule predictions.

However, we cannot exclude alternative solutions with significant contributions from $N^*(1900)$ or $N^*(1650)$, although there are some arguments favoring the solution with the dominant $N^*(1535)$ contribution. For a better understanding of the dynamics of these reactions, more experimental data at other excess energies with Dalitz plots and angular distributions are desired.

ACKNOWLEDGMENTS

We thank Feng-kun Guo, Bo-chao Liu, Colin Wilkin, Feng-quan Wu, and Hai-qing Zhou for useful discussions. This work is partly supported by the National Natural Science Foundation of China under grant nos. 10435080 and 10521003 and by the Chinese Academy of Sciences under project no. KJCX3-SYW-N2.

-
- [1] C. Hanhart, Phys. Rep. **397**, 155 (2004).
 [2] B. S. Zou, Int. J. Mod. Phys. A **21**, 835 (2006) and references therein.
 [3] S. Okubo, Phys. Lett. **5**, 165 (1963); G. Zweig, CERN report Th-412 (1964); J. Iizuka, Prog. Theor. Phys. Suppl. **38**, 21 (1966).
 [4] F. Balestra *et al.* (DISTO Collaboration), Phys. Rev. Lett. **81**, 4572 (1998); Phys. Rev. C **63**, 024004 (2001).
 [5] M. Hartmann *et al.*, Nucl. Phys. **A755**, 459c (2005).
 [6] A. Sibirtsev, J. Haidenbauer, and U.-G. Meisser, Eur. Phys. J. A **27**, 263 (2006); A. Sibirtsev and W. Cassing, *ibid.* **7**, 407 (2000).
 [7] A. I. Titov, B. Kämpfer, and B. L. Reznik, Eur. Phys. J. A **7**, 543 (2000).
 [8] K. Nakayama, in *Proceedings of the Symposium on "Threshold meson production in pp and pd interaction"* at Cracow 2001, Schriften des Forschungszentrums Juelich, Matter and Materials, edited by P. Moskal and M. Wolke, Vol. 11, pp. 119–146 (2002); K. Tsushima and K. Nakayama, Phys. Rev. C **68**, 034612 (2003).
 [9] L. P. Kaptari and B. Kämpfer, Eur. Phys. J. A **23**, 291 (2005).
 [10] M. Hartmann *et al.*, Phys. Rev. Lett. **96**, 242301 (2006).
 [11] B. C. Liu and B. S. Zou, Phys. Rev. Lett. **96**, 042002 (2006); **98**, 039102 (2007); B. C. Liu and B. S. Zou, Commun. Theor. Phys. **46**, 501 (2006).
 [12] G. Penner and U. Mosel, Phys. Rev. C **66**, 055211 (2002); **66**, 055212 (2002); V. Shklyar, H. Lenske, and U. Mosel, *ibid.* **72**, 015210 (2005).
 [13] B. Julia-Diaz, B. Saghai, T. S. H. Lee, and F. Tabakin, Phys. Rev. C **73**, 055204 (2006).
 [14] M. Q. Tran *et al.*, Phys. Lett. **B445**, 20 (1998); K. H. Glander *et al.*, Eur. Phys. J. A **19**, 251 (2004).
 [15] J. W. C. McNabb *et al.*, Phys. Rev. C **62**, 042201(R) (2004).
 [16] T. Inoue, E. Oset, and M. J. Vicente Vacas, Phys. Rev. C **65**, 035204 (2002); N. Kaiser, T. Waas, and W. Weise, Nucl. Phys. **A612**, 297 (1997).
 [17] M. Dugger *et al.*, Phys. Rev. Lett. **96**, 062001 (2006); Erratum-*ibid.* **96**, 169905 (2006).
 [18] R. Machleidt, K. Holinde, and C. Elster, Phys. Rep. **149**, 1 (1987); R. Machleidt, Adv. Nucl. Phys. **19**, 189 (1989); R. Brockmann and R. Machleidt, Phys. Rev. C **42**, 1965 (1990).
 [19] K. Tsushima, S. W. Huang, and A. Faessler, Phys. Lett. **B337**, 245 (1994); K. Tsushima, A. Sibirtsev, and A. W. Thomas, *ibid.* **B39**, 29 (1997); K. Tsushima, A. Sibirtsev, A. W. Thomas, and G. Q. Li, Phys. Rev. C **59**, 369 (1999); Erratum-*ibid.* **61**, 029903 (2000).

- [20] A. Sibirtsev and W. Cassing, nucl-th/9802019; A. Sibirtsev, K. Tsushima, W. Cassing, and A. W. Thomas, Nucl. Phys. **A646**, 427 (1999).
- [21] W. Grein and P. Kroll, Nucl. Phys. **A338**, 332 (1980); M. Kirchbach and L. Tiator, Nucl. Phys. **A604**, 385 (1996); S. L. Zhu, Phys. Rev. C **61**, 065205 (2000).
- [22] G. Fäldt and C. Wilkin, Phys. Scr. **64**, 427 (2001).
- [23] B. S. Zou and F. Hussain, Phys. Rev. C **67**, 015204 (2003).
- [24] Particle Data Group, J. Phys. G **33**, 1 (2006).
- [25] T. P. Vrana, S. A. Dytman, and T. S. H. Lee, Phys. Rep. **328**, 181 (2000).
- [26] X. Q. Li, D. V. Bugg, and B. S. Zou, Phys. Rev. D **55**, 1421 (1997).
- [27] T. Feuster and U. Mosel, Phys. Rev. C **58**, 457 (1998); **59**, 460 (1999).
- [28] W. H. Liang, P. N. Shen, J. X. Wang, and B. S. Zou, J. Phys. G **28**, 333 (2002).
- [29] A. Baldini, V. Flamino, W. G. Moorhead, and D. R. O. Morrison, *Total Cross Sections of High Energy Particles: Landolt-Börnstein, Numerical Data and Functional Relationships in Science and Technology*, edited by H. Schopper (Springer-Verlag, New York, 1988), Vol. 12.
- [30] J. Gillespie, *Final-State Interactions*, Holden-Day Advanced Physics Monographs (1964).
- [31] M. Batinić, A. Svarc, and T. S. H. Lee, Phys. Scr. **56**, 321 (1997).
- [32] K. Nakayama, J. Speth, and T. S. H. Lee, Phys. Rev. C **65**, 045210 (2002); K. Nakayama, J. W. Durso, J. Haidenbauer, C. Hanhart, and J. Speth, Phys. Rev. C **60**, 055209 (1999).
- [33] G. Gedalin, A. Moalem, and L. Razdolskaja, Nucl. Phys. **A634**, 368 (1998).
- [34] L. Hannelius and D. O. Riska, Phys. Rev. C **62**, 045204 (2000).
- [35] J. Ellis, M. Karliner, D. E. Kharzeev, and M. G. Sapozhnikov, Nucl. Phys. **A673**, 256 (2000).
- [36] H. Gao, T. S. H. Lee, and V. Marinov, Phys. Rev. C **63**, 022201(R) (2001).
- [37] F. Huang, Z. Y. Zhang, and Y. W. Yu, Phys. Rev. C **73**, 025207 (2006).
- [38] A. Zhang *et al.*, High Energy Phys. Nucl. Phys. **29**, 250 (2005).